British Journal of Pharmacology (2005) 146, 1000–1009
www.nature.com/bjp

Analysis of macroscopic ionic currents mediated by GABAρ_1 receptors during lanthanide modulation predicts novel states controlling channel gating

[1]Juan D. Goutman, [2]Ariel L. Escobar & *,[1]Daniel J. Calvo

[1]Laboratorio de Neurobiología Celular y Molecular, Instituto de Investigaciones en Ingeniería Genética y Biología Molecular (INGEBI), Consejo Nacional de Investigaciones Científicas y Técnicas (CONICET), Departamento de Fisiología, Biología Molecular y Celular, Facultad de Ciencias Exactas y Naturales (FCEyN), Universidad de Buenos Aires (UBA), Vuelta de Obligado 2490, CP 1428 Ciudad Autónoma de Buenos Aires, Argentina and [2]Department of Physiology, Texas Tech University Health Sciences Center, Lubbock, TX 79430-6551, U.S.A.

1 Lanthanide-induced modulation of $GABA_C$ receptors expressed in *Xenopus* oocytes was studied.

2 We obtained two-electrode voltage-clamp recordings of ionic currents mediated by recombinant homomeric GABAρ_1 receptors and performed numerical simulations of kinetic models of the macroscopic ionic currents.

3 GABA-evoked chloride currents were potentiated by La^{3+}, Lu^{3+} and Gd^{3+} in the micromolar range.

4 Lanthanide effects were rapid, reversible and voltage independent.

5 The degree of potentiation was reduced by increasing GABA concentration.

6 Lu^{3+} also induced receptor desensitization and decreased the deactivation rate of GABAρ_1 currents.

7 In the presence of 300 μM Lu^{3+}, dose–response curves for GABA-evoked currents showed a significant enhancement of the maximum amplitude and an increase of the apparent affinity.

8 The rate of onset of TPMPA and picrotoxin antagonism of GABAρ_1 receptors was modulated by Lu^{3+}.

9 These results suggest that the potentiation of the anionic current was the result of a direct lanthanide–receptor interaction at a site capable of allosterically modulating channel properties.

10 Based on kinetic schemes, which included a second open state and a nonconducting desensitized state that closely reproduced the experimental results, two nonexclusive probable models of GABAρ_1 channels gating are proposed.

British Journal of Pharmacology (2005) **146,** 1000–1009. doi:10.1038/sj.bjp.0706411;
published online 10 October 2005

Keywords: GABA; $GABA_C$ receptors; cationic modulation; chloride channels; lanthanides; kinetic modeling; human retina; *Xenopus* oocytes

Abbreviations: Cl^-, chloride; GABA, γ-aminobutyric acid; *I–V*, current–voltage; HEPES, 4-(2-hydroxyethyl)-1-piperazineethanesulfonic acid

Introduction

Ligand-gated ion channels can be modulated by many cations through actions exerted on diverse protein domains including the pore (Dodge *et al*., 1969; Miledi & Parker, 1980; Smart & Constanti, 1982; Squires & Saederup, 1982; Mayer *et al*., 1984; Narahashi *et al*., 1994). Different inorganic cations modulate neurotransmitter actions on γ-aminobutyric acid (GABA), glutamate, acetylcholine and other synaptic receptors (Mayer *et al*., 1984; Reichling & Macdermott, 1991; Ma *et al*., 1993b; Laube *et al*., 1995; Galzi *et al*., 1996; Garcia-Colunga & Miledi, 1997; Acuna-Castillo *et al*., 2000; Mott *et al*., 2003) by altering ligand-binding affinity, ionic channel gating and other parameters (Miledi & Parker, 1980; Ma *et al*., 1994; Hackos & Korenbrot, 1997; Barberis *et al*., 2000; Mozrzymas *et al*., 2003).

*Author for correspondence; E-mail: dcalvo@dna.uba.ar

$GABA_A$ and $GABA_C$ receptors are chloride (Cl^-) channels (Moss & Smart, 2001) sensitive to both exogenous and endogenous cations (Arakawa *et al*., 1991; Calvo *et al*., 1994; Qian *et al*., 1997; Fisher & Macdonald, 1998; Hosie *et al*., 2003). For example, Zn^{2+} and other divalent cations inhibit responses mediated by these ionotropic GABA receptors (Smart & Constanti, 1982; Westbrook & Mayer, 1987; Draguhn *et al*., 1990; Legendre & Westbrook, 1991; Smart, 1992; Calvo *et al*., 1994; Chang *et al*., 1995), whereas lanthanides potentiate them (Im *et al*., 1992; 1993; Ma & Narahashi, 1993a; Ma *et al*., 1993b; 1994; Calvo *et al*., 1994; Narahashi *et al*., 1994; Saxena *et al*., 1997; Zhu *et al*., 1998).

Lanthanides, which are trivalent cations with chemical and biological properties similar to alkaline earth elements, include a series of 15 metals in the periodic table, from lanthanum (La^{3+}, atomic number 57) to lutetium (Lu^{3+}, atomic number

71) (Ma & Narahashi, 1993a). The allosteric nature of lanthanide modulation of $GABA_A$ has been described (Calvo *et al*., 1994; Narahashi, 2000). Potentiating effects of diverse lanthanides on homomeric $GABA_C$ receptors composed of ρ_1 subunits were also found (Calvo *et al*., 1994). In the present work, we tested the hypothesis that lanthanides modify the gating of $GABA_C$ receptors. A detailed study of the effects of Lu^{3+} on GABAρ_1 receptors was performed and compared with the actions of La^{3+} and Gd^{3+}. The mechanism underlying Lu^{3+} actions was evaluated by obtaining dose–response curves for GABA, kinetic measurements of the ionic currents, and by observing the effects of competitive and noncompetitive $GABA_C$ receptor antagonists in the presence or absence of this lanthanide. Based on these results, we propose two probable kinetic schemes that account for the lanthanide-GABAρ_1 receptor interaction. Both schemes required a second open state as well as a new desensitized state for GABAρ_1 channels.

Methods

RNA preparation, oocyte isolation and cell injection

A human cDNA encoding the ρ_1 $GABA_C$ receptor subunit cloned in the vector pBS (SK^-) (Promega, Madison, WI, U.S.A.), suitable for *in vitro* transcription, was used as a template to synthesize cRNAs. cRNA solutions (0.1–0.3 ng nl^{-1}) were prepared in RNase-free H_2O and stored at −70°C.

Xenopus laevis (Nasco, Modesto, CA, U.S.A.) oocytes at stages V and VI were used for expression of exogenous cRNAs. Isolation and maintenance of cells were carried out as previously described (Miledi *et al*., 1989). Briefly, frogs were anesthetized with 3-aminobenzoic-acid ethylester (1 g ml^{-1}) and ovaries were surgically removed. Ovaries were incubated with 200 U ml^{-1} collagenase for 50 min at room temperature (RT) and isolated oocytes were maintained in an incubator at 17°C in Barth's medium (in mM: 88 NaCl; 0.33 $Ca(NO_3)_2$; 0.41 $CaCl_2$; 1 KCl; 0.82 $MgSO_4$; 2.4 $NaHCO_3$; 10 HEPES and 0.1 mg ml^{-1} gentamycin; pH was adjusted to 7.4 with NaOH). After 1 day, each oocyte was manually microinjected (microinjector Drummond Sci. Co., Broomall, PA, U.S.A.) with 50 nl of a solution containing 5–15 ng of cRNA.

All experiments were carried out according to NIH guidelines for the care and use of laboratory animals.

Electrophysiological recordings

$GABA_C$ channels show a very small single channel conductance and a high open probability that preclude a classical analysis of single channel kinetics (Wotring *et al*., 1999). Specifically, small amplitude single ionic currents need to be heavily filtered in order to be idealized. This filtering produces an important time correlation of the temporal realization of the Markov chain that describes the single channel behavior (Rosales *et al*., 2004) and making the data to lose the memory less condition necessary to critically evaluate any kinetic model associated with a Markov process (Rosales *et al*., 2004). Thus, we conducted two-electrode voltage-clamp recordings of ionic currents and performed numerical simulations of kinetic models of the macroscopic ionic currents (see below).

Two-electrode voltage-clamp recordings were performed with an Axoclamp 2B amplifier (Axon Instruments, Union City, CA, U.S.A.) 3–7 days after oocyte injection. Standard glass recording electrodes were made in a Narishige PB-7 puller (Narishige Scientific Instrument Lab., Tokyo, Japan) and filled with 3 M KCl. Resistance values were approximately 1 MΩ. Holding potential was set to −70 mV, and current traces were acquired with an analog to digital interface (Labmaster TL-1 DMA, Scientific solutions Inc., Solon, OH, U.S.A.) and stored on a PC using AXOTAPE software (Axon Instruments).

Cells were placed in a chamber (volume 100 μl) and continuously superfused (12 ml min^{-1}) with frog Ringer's solution (in mM: 115 NaCl; 2 KCl; 1.8 $CaCl_2$; 5 HEPES; pH 7.0). GABA and other compounds were applied through the perfusion system. The speed of solution exchange was measured as follows: an oocyte expressing GABAρ_1 receptors was placed in the recording chamber and a response was evoked with a low concentration of agonist. Once the current reached a maximum, a low Cl^- Ringer's solution (in mM: 65 NaCl; 2 KCl; 1.8 $CaCl_2$; 1.8 $MgCl_2$; 50 methane sulfonic acid; 5 HEPES; pH 7.0) was applied through the perfusion system without changing the GABA concentration. Next, the time required for equilibration after the change in the current driving force was measured. Complete solution exchange ($\approx$95%) was achieved in less than 4 s. All the experiments were carried out at RT (23–24°C).

Test solutions: different concentrations of lanthanide chloride salts were added to the solutions that contained HEPES. The pH of each solution was always checked and adjusted as necessary. These solutions presented some practical problems. Although lanthanides are predominantly trivalent cations, coordination numbers in the lanthanide series of elements are highly flexible; therefore, it was unavoidable that smaller amounts of other valence states (especially the divalent hydroxides) were present in the solutions. To avoid the formation of insoluble hydroxides, the lanthanide stock solutions were kept slightly acidified and stored in plastic containers to prevent binding of the lanthanides to negative charges of glass (Reichling & Macdermott, 1991). Estimates of lanthanide concentrations in the millimolar range are potentially unreliable because they may polymerize in concentrated aqueous solutions.

Materials

The transcription kit mMessage mMachine was purchased from Ambion (Austin, TX, U.S.A.), and Type I collagenase was obtained from Worthington (Freehold, NJ, U.S.A.). Picrotoxin, 1,2,5,6-tetrahydropyridine-4-yl methylphosphinic acid (TPMPA), all the salts, HEPES, 3-aminobenzoic-acid ethylester, RNase-free H_2O and dimethyl sulfoxide (DMSO) were purchased from Sigma-Aldrich (St Louis, MO, U.S.A.).

Data analysis

Data were analyzed with Origin v. 6.0 (MicroCal, Northampton, MA, U.S.A.). Statistical analyses were performed using a two tailed Student's *t*-test. Kinetic studies were performed by calculation of the selected deactivation ($t_{deact10–90\%}$) and inhibition constants ($t_{inh10–90\%}$) for current ensembles (averaged traces), where $t_{deact10–90\%}$ represented the time

required to go from 10 to 90% of the whole current deactivation process, and $t_{inh10-90\%}$ represented the time required to go from 10 to 90% of the current inhibition.

Dose–response (D–R) curves were fit by the logistic equation $I_{max} = B\{1-1/[1+(A/EC_{50})^n]\}$, where A is the agonist concentration, B is the maximal response, EC_{50} is the concentration of agonist that elicits half maximal responses, and n is the Hill coefficient.

Modeling GABAρ_1 currents

Ionic currents mediated by GABAρ_1 receptors were simulated by integrating the mass-action law differential equations that correspond to the kinetic scheme indicated in Figure 6. The differential equations were written in a matricial form and integrated using the Q matrix formalism (Colquhoun & Hawkes, 1981; 1982). Briefly, following standard theory,

$$\frac{d\boldsymbol{p}(t)}{dt} = \boldsymbol{p}(t)\boldsymbol{Q} \quad (1)$$

with $\boldsymbol{Q}$ as a matrix with elements q_{ij}. If $\boldsymbol{p}(0)$ is the steady state vector for initial conditions

$$\boldsymbol{p}(t) = \boldsymbol{p}(0)e^{\boldsymbol{Q}t} \quad (2)$$

with $e^{\boldsymbol{Q}t}$ as the matrix exponential (Colquhoun & Hawkes, 1977; 1982).

Steady-State probabilities

Under steady-state conditions, the probability for each state can be expressed as

$$\boldsymbol{p}(\infty) = \boldsymbol{u}(\boldsymbol{S}\boldsymbol{S}^{T})^{-1} \quad (3)$$

where $\boldsymbol{p}(\infty)$ is a $1 \times m$ vector whose elements are the probabilities of being in each state at the equilibrium condition. $\boldsymbol{u}$ denotes a unitary $1 \times m$ vector and $\boldsymbol{S}$ a $(m+1) \times m$ matrix obtained by expanding $\boldsymbol{Q}$ with a column unitary vector of dimension $m \times 1$ and $\boldsymbol{S}^{T}$ the transposed matrix (Colquhoun & Hawkes, 1995). The simulation process starts by sampling the initial state from $\boldsymbol{p}(\infty)$.

Results

Modulation by lanthanides of GABA-induced Cl^- currents

Figure 1 illustrates responses elicited by 3 μM GABA in oocytes injected with the ρ_1 subunit. Once the GABA-induced current reached a plateau, the oocytes were superfused with 1 mM lanthanides. La^{3+}, Lu^{3+} and Gd^{3+} increased the amplitude of GABA-induced Cl^- currents (Figure 1a, b and c); however, GABA-induced Cl^- currents kinetics and the observed rebound currents upon washout differed depending on the particular lanthanide. La^{3+} potentiation of GABA-induced Cl^- currents was rapid, stable and fully reversible after washout (Figure 1a), whereas the effects of Lu^{3+} and Gd^{3+} were more complex and comprised of a biphasic time course. Lu^{3+} and Gd^{3+}, applied during the GABA response, induced rapid increases in GABA-induced Cl^- currents but, unlike La^{3+}, did not produce an immediate steady-state response. Instead, the current reached a maximum and rapidly declined (Figure 1b and c). Once Lu^{3+} or Gd^{3+} was removed, a rebound current was observed. This rebound was also reversible and depended on GABA concentration. For example, Lu^{3+} potentiation of responses elicited by 1 μM GABA, a concentration around the EC_{50}, underwent significant decrease over the time of lanthanide application (Figure 2), whereas responses to lower concentrations of GABA (0.3 μM) did not decline (Figure 2). Meanwhile, applications of 0.3 or 1 μM GABA alone did not induce any current desensitization. In addition, responses evoked by a different agonist such as β-alanine (1 mM; concentration value

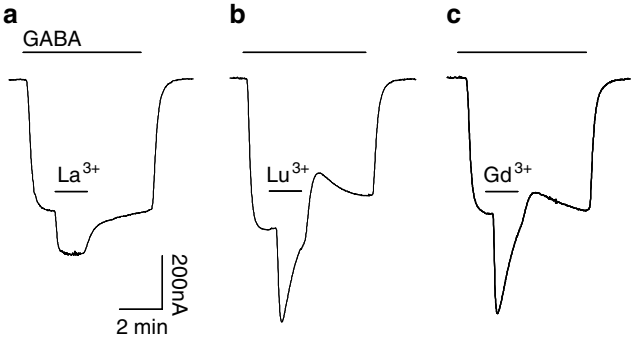

Figure 1 Potentiation of GABA-induced Cl^- currents by lanthanides. (a) Representative trace of an ionic current elicited by 3 μM GABA and potentiated by 1 mM La^{3+}. La^{3+} was applied during the maximum response to GABA. The effect was sustained during the presence of lanthanide and fully reversible. (b and c) Same experiment as shown in (a) but 1 mM Lu^{3+} (b) or 1 mM Gd^{3+} (c) was applied instead of La^{3+}. The time course for lanthanide action in (b and c) differed from that observed in (a). The fast initial increase in current amplitude was followed by a rapid decrease of the effect in the presence of lanthanide (and GABA). After removing the lanthanide (b and c), a rebound was observed.

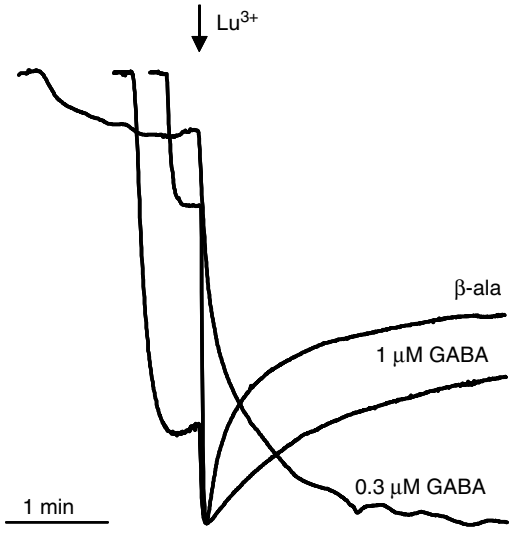

Figure 2 Lu^{3+}-induced GABA-activated Cl^- currents potentiation depends on the type and concentration of agonist used. Representative currents evoked by 0.3 and 1 μM GABA or 1 mM β-alanine, recorded in the same oocyte, were superimposed to compare time courses after a 1 mM Lu^{3+} application, and their amplitudes were normalized. Desensitization of GABAρ_1 responses was more prominent for the higher GABA concentration and for currents evoked by β-alanine.

around the EC_{50} and nondesensitizing as well) (Calvo & Miledi, 1995) showed a more pronounced decline (Figure 2).

This Lu^{3+} induced current desensitization was dependent on both the type of agonist used (GABA or β-alanine) and also on the concentration. This suggests that lanthanide's effects were due to a direct cation-receptor interaction. Since different lanthanides showed different actions on homomeric GABAρ_1 receptors, we decided to use Lu^{3+} and further analyze the mechanisms underlying this modulation.

D–R analysis and current–voltage relationship

We have previously demonstrated that La^{3+} shifted the D–R curve for GABA to the left without a substantial change in the maximal response (Calvo *et al*., 1994). These results indicated an increase in the apparent affinity of GABAρ_1 receptors. Lu^{3+} also shifted the D–R curve to the left but in addition increased the maximal response to GABA (Figure 3a). Potentiation of GABA 10 and 100 μM responses by 300 μM Lu^{3+} reached 19.3 ± 4.7 and $20.1\pm1.0\%$ ($n=9$) respectively. A significant increase in the apparent affinity of GABAρ_1 receptors for GABA was also observed in the presence of 300 μM Lu^{3+}. In agreement with previous reports, the EC_{50} for GABA was 0.7 ± 0.1 μM, with a Hill coefficient of 2.2 ± 0.2. In the presence of 300 μM Lu^{3+}, EC_{50} was 0.4 ± 0.1 μM ($P<0.05$), with a Hill coefficient of 1.6 ± 0.2. Figure 3b shows the potentiation of 1 μM GABA responses produced by different concentrations of Lu^{3+}. Saturating doses could not be tested because Lu^{3+} solutions above 1 mM showed poor solubility and raised the possibility of complex precipitation (see Methods). For 1 mM Lu^{3+} the maximum potentiation observed was $115.7\pm1.9\%$ ($n=9$).

As mentioned above, Lu^{3+} effects depended strongly on GABA concentration (Figure 3c). The Lu^{3+} potentiation of currents evoked by low (0.3–1 μM) concentrations of GABA was greater than 50%, but only 20% and approximately constant for higher concentrations (20–100 μM). In addition, neither Lu^{3+}, La^{3+} nor Gd^{3+} (1 mM) were able to activate GABAρ_1 receptors in the absence of GABA. For example, 1 mM Lu^{3+} induced negligible current in oocytes expressing GABAρ_1 receptors (5.2 ± 0.3 nA, $n=3$). Such current did not significantly differ from that evoked in water-injected oocytes exposed to Lu^{3+} (4.5 ± 0.3 nA, $n=3$; $P>0.05$).

Figure 3d illustrates the *I–V* relationships obtained under control conditions (1 μM GABA) or with the addition of 300 μM Lu^{3+}. The increase in GABA-induced Cl^- currents was independent of the holding potential, and the reversal potential was unaffected by Lu^{3+}. These results agreed with previous observations of lanthanides acting on $GABA_A$ and $GABA_C$ receptors (Ma *et al*., 1993b; Calvo *et al*., 1994).

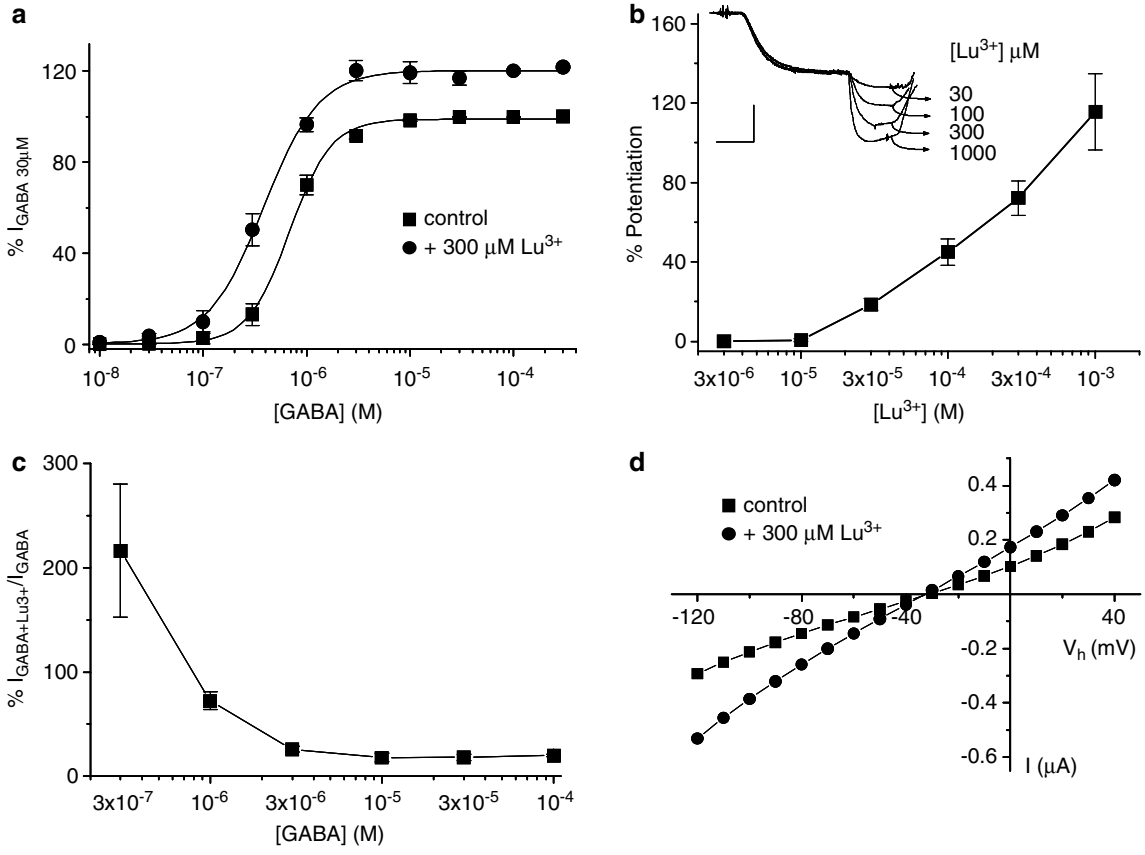

Figure 3 Analysis of Lu^{3+} effects on GABAρ_1 receptors. (a) Dose–response curves for GABA in the presence or absence of 300 μM Lu^{3+}. Response amplitudes were expressed as fraction of 30 μM GABA-evoked currents. (b) Potentiation of GABA-induced Cl^- currents exerted by different concentrations of Lu^{3+}. Data were obtained by normalizing the current amplitude to control responses (1 μM GABA). Inset: Superimposed current traces showing the effects of increasing concentrations of Lu^{3+} on currents evoked by 1 μM GABA in a representative experiment. (c) GABA concentration dependence of the Lu^{3+} potentiation of GABA-induced Cl^- currents. (d) *I–V* relationship for GABAρ_1 responses evoked by 1 μM GABA in the presence or absence of 300 μM Lu^{3+}.

Deactivation of GABAρ$_1$ currents during lanthanide modulation

D–R curves define the parameters of steady-state modulation. We investigated nonsteady-state conditions to determine more precisely the gating scheme for this receptor (see below). Figure 4 illustrates the Lu^{3+} (1 mM) modulation of GABAρ_1 responses evoked by 1 μM GABA. The two current traces were superimposed to illustrate the effect of this lanthanide on GABAρ_1 receptor deactivation. The dotted trace shows a control experiment similar to the one in Figure 1b, but in this case Lu^{3+} and GABA were promptly and simultaneously removed once the current approached a peak. The $t_{deact10–90\%}$ was 32.0 ± 7.0 s ($n=3$). Lu^{3+} appreciably slowed the response relaxation, when GABA was removed from the bath (Figure 4, solid trace): $t_{deact10–90\%}$ was 183.0 ± 31.0 s ($n=3$, $P<0.05$). As will be discussed later during the description of the model, Lu^{3+} would increase the probability of channels reopening occurrence during the response deactivation, reducing its overall rate constant.

Lu^{3+} modulation of TPMPA and picrotoxin actions on GABAρ$_1$ receptors

To further analyze the nature of Lu^{3+} actions on GABAρ_1 receptors, we studied the effects of this lanthanide on the degree of inhibition and time course of action of two $GABA_C$ receptor antagonists. The ability of the competitive antagonist TPMPA (Ragozzino *et al*., 1996), and the noncompetitive antagonist picrotoxin (Woodward *et al*., 1992; Wang *et al*., 1995; Goutman & Calvo, 2004) to inhibit responses mediated by GABAρ_1 receptors was evaluated in the presence or absence of Lu^{3+}. Figure 5a shows the effect of TPMPA on GABA-induced Cl^- currents during the application of Lu^{3+}.

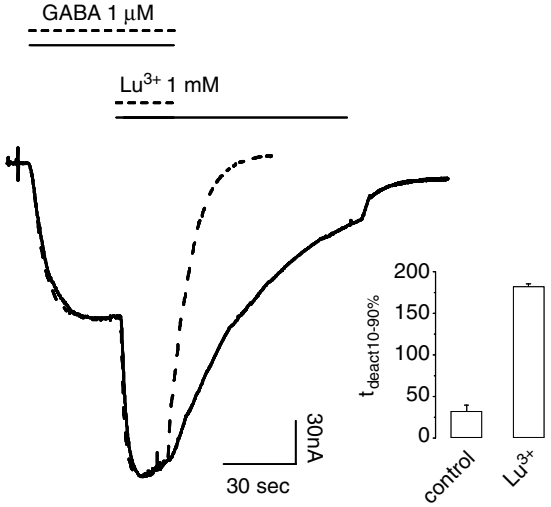

Figure 4 Lanthanide-induced slowing of GABA-induced Cl^- currents deactivation. Representative recordings illustrating the effect of 1 mM Lu^{3+} on currents evoked by 1 μM GABA. Dotted current trace: control experiment, Lu^{3+} and GABA were removed (dotted bars represents applications time course) once the current reached a peak. Solid current trace: lanthanide was present during GABA removal from the bath (solid bars represents applications time course). Current traces were superimposed for simplicity. Inset: Deactivation constants measured for control currents or during a constant application of 1 mM Lu^{3+} during GABA washout.

As previously shown in Figure 1, 300 μM Lu^{3+} enhanced GABA-induced Cl^- currents, and this was followed by attenuation in this effect (control experiment, Figure 5a dotted trace). The current evoked in the presence of both GABA and Lu^{3+} was also sensitive to TPMPA (Figure 5a, solid trace). Inhibition produced by 30 μM TPMPA was $90.8 \pm 3.8\%$ ($n=3$), and the time course for antagonism showed a $t_{inh10–90\%} = 107.4 \pm 9.2$ s ($n=3$).

In a similar experiment performed on the same oocyte, 3 μM GABA was applied instead of Lu^{3+}, once the current evoked by 1 μM GABA reached its plateau (Figure 5b, dotted trace). Following a 3-min period of superfusion with 3 μM GABA, oocytes were re-exposed to 1 μM GABA and finally to normal Ringer's, producing complete relaxation of the response (Figure 5b, dotted trace). Current activation levels reached during applications of 3 μM GABA were similar to that observed for responses simultaneously elicited by GABA and Lu^{3+} (shown in Figure 5a). On the other hand, it was observed that little receptor desensitization occurred during GABA superfusion. For example, application of GABA 3 μM produced a maximum decay of $7.8 \pm 1.0\%$ ($n=5$) that reached the plateau in 2 min. Desensitization developed in the presence of Lu^{3+} was more pronounced. The application of 300 μM

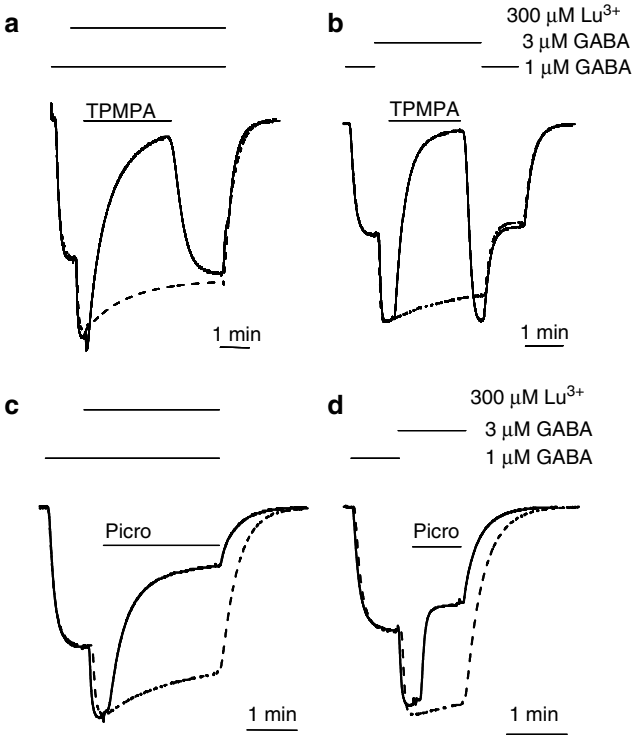

Figure 5 Modulation by Lu^{3+} of GABAρ_1 receptor antagonism. (a) Representative experiments showing the effect of Lu^{3+} on the time course and degree of antagonism exerted by TPMPA on GABA-induced Cl^- currents. In these experiments, 300 μM Lu^{3+} was added alone (dotted trace) or together with 30 μM TPMPA (solid trace) during the plateau of GABA-induced Cl^- currents evoked by 1 μM GABA. (b) Same experiment as shown in (a) but TPMPA antagonism was tested on responses evoked by 3 μM GABA (dotted trace), a concentration that elicited a response equivalent to that obtained by 300 μM Lu^{3+}. (c and d) Same experiments as shown in (a and b) but 3 μM picrotoxin was applied instead of TPMPA. Recovery of GABA-induced Cl^- currents after antagonism was omitted in this protocol.

Lu^{3+} produced a decay of $18.1 \pm 1.7\%$ ($n=5$), but steady state was not attained in the same period of time. The application of 30 μM TPMPA, together with 3 μM GABA (Figure 5b, solid trace), inhibited GABA-induced Cl^- currents by $93.3 \pm 3.7\%$ ($n=3$), which was not significantly different from the inhibition in the presence of Lu^{3+} ($P>0.05$) (Figure 5a). Meanwhile, the rise time for this process was: $t_{inh10-90\%} = 58.5 \pm 7.54$ s ($n=3$), which is about one half as long as that seen with 300 μM Lu^{3+} ($P<0.05$) (Figure 5a). GABA-evoked currents observed immediately after TPMPA removal (solid trace) were larger than currents recorded in the absence of TPMPA and at the end of 3 μM GABA application (dotted trace). This was most likely due to a preventive effect exerted by TPMPA on (GABA-induced) GABAρ_1 receptor desensitization. This action of TPMPA resembled previously described bicuculline effects on $GABA_A$ receptors, which were observed in similar experiments (Bianchi & Macdonald, 2001), and confirmed the competitive nature of TPMPA, as previously reported (Ragozzino *et al*., 1996). Protective effects of TPMPA on receptor desensitization were not observed for currents modulated by Lu^{3+} (Figure 5a), suggesting a distinctive process during the action of this lanthanide.

The effect of Lu^{3+} on picrotoxin antagonism of GABAρ_1 receptors was evaluated through a similar approach. Figure 5d depicts a representative experiment showing the effect of 3 μM picrotoxin on currents elicited by 3 μM GABA. The degree of picrotoxin antagonism was $41.0 \pm 10.2\%$ ($n=4$), with a characteristic time course of $t_{inh10-90\%} = 9.3 \pm 2.1$ s ($n=4$). In the presence of Lu^{3+} (Figure 5c), an inhibition of $57.1 \pm 8.9\%$ ($n=4$) was observed, together with a considerable decrease in the rate of antagonism, $t_{inh10-90\%} = 46.4 \pm 5.7$ s; $n=4$; $P<0.05$. The time to reach maximal levels of antagonism in the course of Lu^{3+} action (Figure 5c) was longer than during the application of 3 μM GABA (Figure 5d), and also significantly longer than the time measured for the completion of picrotoxin inhibition in 1 μM GABA (Figure 5c): $t_{inh10-90\%} = 17.4 \pm 0.1$ s ($n=3$, $P<0.05$).

Due to the fact that the time course for picrotoxin inhibition appeared to depend on the degree of current activation or agonist concentration (Woodward *et al*., 1992; Goutman & Calvo, 2004), it was surprising to find that the extent and time course of inhibition in the presence of Lu^{3+} was different even if the open probability of the GABAρ_1 receptor was the same (see below).

Kinetic model for lanthanide modulation of GABAρ_1 receptors

To more precisely describe the mechanism of action underlying modulation of GABAρ_1 receptors by lanthanides, we performed numeric simulations based on a mathematical model of the channel's activity. A basic scheme was taken from the gating model for GABAρ_1 receptors proposed by Chang & Weiss (1999).

$$3A + R \underset{5k_{on}}{\overset{k_{off}}{\rightleftharpoons}} 2A + AR$$

$$\underset{4k_{on}}{\overset{2k_{off}}{\rightleftharpoons}} A + A_2R \underset{3k_{on}}{\overset{3k_{off}}{\rightleftharpoons}} A_3R \underset{\beta}{\overset{\alpha}{\rightleftharpoons}} A_3R^*$$

In this scheme at least three GABA molecules would be required to activate the receptor, each one participating in individual and consecutive GABA binding steps, followed by a last transition representing the conformational change associated with gating.

Based on the experimental results, we evaluated different gating models capable of reproducing our findings. In order to obtain the closer fit to the results, a few modifications into the Chang–Weiss model were introduced. First, a second open state A_3R^*L was necessary to describe the main features of the Lu^{3+} actions experimentally observed. Additionally, a non-conducting desensitized state (D) was added to explain the temporal decrease observed during Lu^{3+} potentiation (Figure 3a and b). In particular, two kinetic schemes including a second open and a desensitized state were analyzed. Models 1 and 2, illustrated in Figure 6a, were able to describe the experimental findings. In both models, the transition to the second open state (A_3R^*L) would depend on lanthanide concentration ($[L] \times L_{on}$), and the desensitized state would be occupied exclusively from A_3R^*L, implying that it could be populated only in the presence of Lu^{3+}. To simplify the simulation process, the binding of $Lu^{3+}$and the transition to the second open state were modeled as a single step. As our experiments do not provide any piece of information that allowed us to separately determine the binding and the gating steps, we considered this a reasonable simplification. The rate constants values used to carry out the simulations were included in Table 1. The proposed models mainly differ in the step at which Lu^{3+} could bind and gate the second open state and the desensitized state. In model 1 the Lu^{3+} binding step is linked to the closed state A_3R, while in model 2 it is connected to the open state A_3R^*. Both models accurately reproduced the experimental results and did not show significant differences.

Two key characteristics of lanthanide modulation of the GABAρ_1 responses were the increase of peak current and the slower rate of GABA-induced Cl^- current deactivation observed when a lanthanide was present during GABA washout. Thus, we tried to reproduce those features of lanthanide actions on GABAρ_1 receptors by means of kinetic modeling. Figure 6b shows experimental data points (also shown in Figure 3a) of the responses to GABA and 300 μM Lu^{3+} along with simulated responses of Model 1 and 2 (solid and dashed lines of left and right panels, respectively). The simulated peak values are equivalent to those experimentally observed. In the presence of Lu^{3+}, an increase in the peak open probability was observed for both models. In addition, the lanthanide shifted the theoretical GABA D–R curves to the left, as expected.

When simulated peak current values were fit to a Logistic function (not shown), they produced equivalent parameters to those experimentally observed (see Figure 3a). The EC_{50} for GABA (control) was 0.7 ± 0.1 μM, with a Hill coefficient of 1.7 ± 0.1. Meanwhile, simulated D–R curves in the presence of 300 μM Lu^{3+} (not shown) gave the following parameters, Model 1: $EC_{50} = 0.3 \pm 0.1$ μM, Hill coefficient 2.2 ± 0.1, potentiation of a 100 μM GABA response 22%. Model 2: $EC_{50} = 0.3 \pm 0.1$ μM, Hill coefficient 2.2 ± 0.1, potentiation of a 100 μM GABA response 20%.

The kinetic aspects of Lu^{3+} effect were also evaluated with the proposed models. The data illustrated in Figure 6c corresponds to numerical simulations performed with the models 1 and 2. The dotted trace shows the effect of virtual applications of 1 mM Lu^{3+} on top of the simulated responses evoked by 1 μM GABA. The traces replicated the increase in

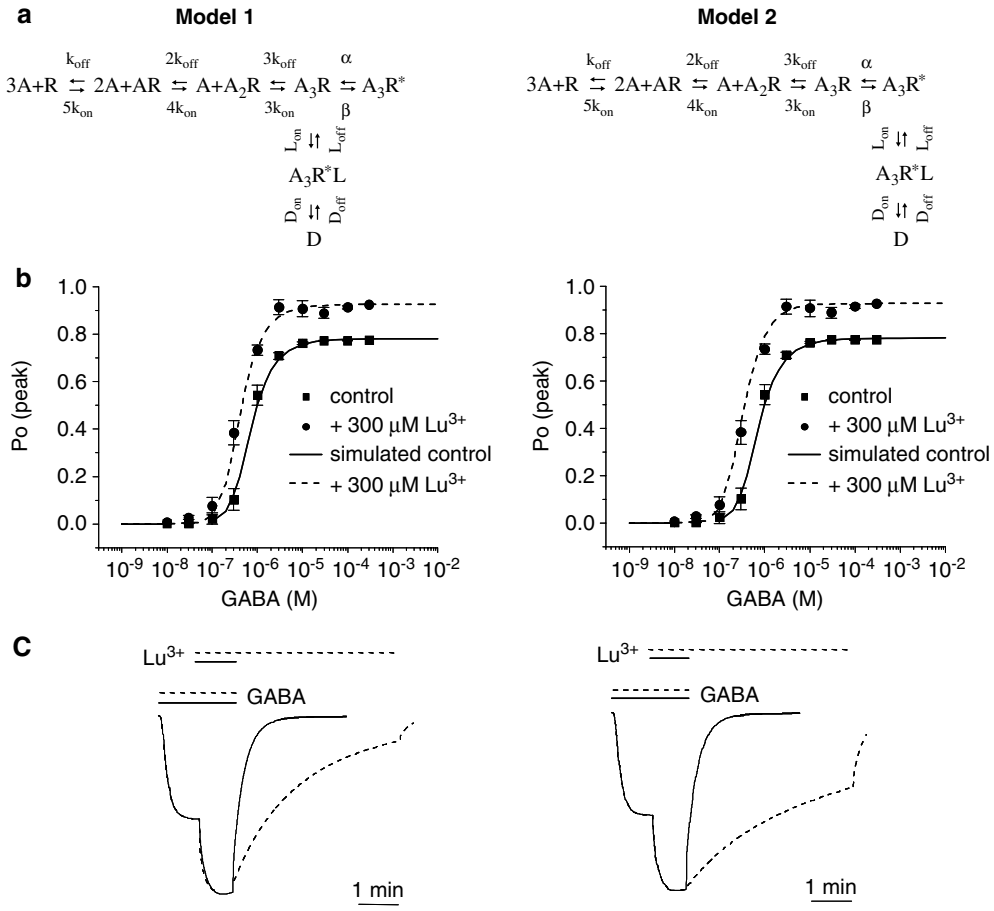

Figure 6 Model of GABAρ_1 receptor gating during lanthanide modulation. (a) Kinetic schemes representing a mechanism for homomeric GABAρ_1 receptor gating during lanthanide action, where A_3R^*L corresponds to a second open state and D represents a desensitized state. Constants describing transitions in the proposed model are listed in the Table 1. (b) Peak open probability (curves) as a function of GABA concentration or GABA plus 300 μM Lu^{3+}. Note that these simulations parallel experimental results (points; control: filled squares, 300 μM Lu^{3+} filled circles, the same as illustrated in Figure 3a). (c) Numeric simulations of the experiment shown in Figure 4. Dotted trace: application of 1 mM Lu^{3+} during 1 μM GABA and deactivation rate after removal of GABA and Lu^{3+}. Solid trace: the model reproduced the slower deactivation time course observed experimentally during a constant application of 1 mM Lu^{3+} during GABA washout.

Table 1 Rate constants for the kinetic models

Rate constant	*Model 1*	*Model 2*
k_{on} ($M^{-1}s^{-1}$)	8×10^4	8×10^4
k_{off} (s^{-1})	0.11	0.11
α (s^{-1})	0.31	0.31
β (s^{-1})	1.11	1.11
L_{on} ($M^{-1}s^{-1}$)	2×10^4	3×10^5
L_{off} (s^{-1})	0.3	15
D_{on} (s^{-1})	3×10^{-3}	3×10^{-3}
D_{off} (s^{-1})	1×10^{-2}	1×10^{-2}

the total anionic current carried through GABAρ_1 receptors during the interaction of lanthanide with the receptor regulatory sites. The dotted trace also shows the rate of deactivation when both, GABA and Lu^{3+}, were simultaneously removed. Interestingly, both proposed models were also able to reproduce the effect of the persistent application of 1 mM Lu^{3+} during GABA washout. These simulations predict a much slower deactivation time course, similar to that observed in Figure 4. Both models produced equivalent results and accurately reproduced the experimental data shown in Figure 4.

Discussion

Two possible kinetic models were proposed to account for the different aspects of the modulation of recombinant homomeric GABAρ_1 receptors by lanthanides. The most evident modulatory effects were displacement of the D–R curve for GABA to lower concentrations and a significant increase in the maximal response (Figure 3a). Additionally, lanthanides significantly slowed GABA-induced Cl^- current deactivation (Figure 4) and also induced receptor desensitization (Figure 2).

The simplest way to explain the shift to the left of the GABA activation curve is to assume that lanthanides diminish the energy barrier for GABA activation. This could be achieved by modification of the GABA binding sites. For example, lanthanides could bind to one or more sites capable of allosterically modulating single-channel properties or increasing the affinity for the agonist. This supposition is consistent with the fact that the sensitivity of GABAρ_1 receptors to competitive and noncompetitive antagonists was also enhanced by Lu^{3+} (Figure 5). A second possibility is that lanthanides might modulate the transition between the

first open state and the last GABA-bound closed state. However, the fact that channel deactivation from the open states was slower in the presence of lanthanides (Figure 4) suggests that these two hypotheses are incomplete. A third and more appealing possibility is that, in the presence of lanthanides, the channels progress to a second open state in which the receptor is more comfortable. That is the channel has a lower energy conformation and, therefore, a higher open probability. Thus, based on the experimental evidence, we postulate new kinetic schemes to explain the interaction of GABA-gated ion channels with lanthanides.

Several schemes, including a second open and a desensitized state, were considered. The two models shown in Figure 6a had the best performance in terms of the Lu^{3+} action on GABA D–R curves and the different observed kinetic features. The main reason to discard a model with a second open state arising from any closed state different from A_3R was the impossibility to simulate the increase in maximal response for a saturating concentration of agonist (Figure 3a). We introduced two additional kinetic states and changed some of the rate constants of the previously proposed scheme (Chang & Weiss, 1999). This kinetic scheme was characterized by two open states independently linked to the triple liganded closed state. The values of α and β reported by Chang and Weiss predicted a $P_{o,max}=[\beta/(\alpha+\beta)]=0.92$. In spite of the fact it was only demonstrated for $GABA_A$ receptors (Ma *et al*., 1994), if we assume that lanthanides do not affect the single conductance ($\cong$1 pS), Lu^{3+}-induced increases in GABA-induced Cl^- current greater than 8% (for maximun responses to GABA in the presence of Lu^{3+} and a $P_{o,max}$ of 0.92) would not be realistic. Because we found increases of approximately a 23% in the D–R curve maximal values during lanthanide modulation, a $P_{o,max}$ of 0.77 was selected. For this purpose, we used the value of α that Chang and Weiss estimated from single-channel data of $GABA_C$ receptors expressed in *Xenopus* oocytes (Chang & Weiss, 1999), whereas β was adjusted to satisfy the new value of $P_{o,max}$. However, it is important to point out that there were no major changes in the simulations when either α or β values were modified (not shown). The rate constants k_{on} and k_{off} were determined from the apparent affinity observed for GABA (Figure 3a) and the activation and deactivation kinetics. Similarly, L_{on}, L_{off}, D_{on} and D_{off} of model 1 and model 2 were based on the concentration dependence of the potentiating effect of Lu^{3+} (Figure 3b) and the time course of its action. The values for k_{on}, k_{off}, α and β were considered unaltered in the presence of lanthanide. Nevertheless, the dissociation rate constant from the second open state (L_{off}) was not very different from the backward rate constant (α) from the GABA activated open state. This suggests that, in the presence of lanthanide, the slowness of deactivation could be explained by reopenings to this second open state.

Potentiation by La^{3+} was fast, stable and fully reversible, whereas the effects of Lu^{3+} and Gd^{3+} showed a more complex time course involving a drop and rebound (Figure 1a–c). Nevertheless, the differences among lanthanides can be most likely explained by variations in the rates of interaction with GABAρ_1 receptor binding sites rather than the existence of diverse mechanisms of action. A more conceivable interpretation of the temporal decrease developed during $Lu^{3+}$and Gd^{3+} potentiation is a lanthanide-dependent desensitization process. The experiments illustrated in Figure 2 agree with this idea, because the rate of desensitization observed in the presence of Lu^{3+} differed for the two agonists tested (GABA and β-alanine). A direct blockage of the channel pore was dismissed based on structural evidence. For example, anionic channels of this family have a vestibule containing series of rings with a high density of positive charge that would decrease the likelihood of interactions with cations (Wotring *et al*., 1999), especially trivalent cations such as lanthanides.

An additional GABA-induced desensitized state was disregarded in this model due to the tiny decrease in amplitude observed for macroscopic GABAρ_1 currents, during long GABA applications (Polenzani *et al*., 1991; Feigenspan *et al*., 1993; Chang & Weiss, 1999). Desensitization produced in the presence of Lu^{3+} showed a different degree and time course than that induced by GABA alone (Figure 5a vs Figure 5b, dotted traces), and was not protected by TPMPA (Figure 5a). These results indicate that the attenuation developed during Lu^{3+} application reflects a singular desensitization process.

Lanthanide effects on GABAρ_1 receptors were independent of the membrane potential. This suggests that the site of action sensed little or none of the transmembrane electrical gradient and implies that lanthanides do not bind to a site within the channel pore. In addition, the fast onset and offset of lanthanide actions suggest an extracellular superficial site. These results agree with previous observations for $GABA_A$ receptors suggesting a distinct site of modulation, different from the GABA binding site (Ma & Narahashi, 1993a; Ma *et al*., 1994; Saxena *et al*., 1997).

Indirect or nonspecific mechanisms underlying the modulation of GABAρ_1 receptors by lanthanides are unlikely. GABA is poorly ionized at physiological pH (negative at pH = 7.3). Therefore, agonist–receptor interactions would be largely independent of the possible screening of fixed negative charges induced by lanthanides (Ma & Narahashi, 1993a). Thus, we have assumed that the effective concentration of ligand remained unchanged. Increases in the maximal responses observed in D–R curves for GABA are consistent with this idea. Lanthanide actions mediated through intracellular signaling systems are also improbable, because the effects were fast, easily reversible and dependant on GABA concentration and the type of agonist used (Figures 2 and 3c). The speed and reversibility of the lanthanide effects also suggest that they were not due to entry of these trivalent cations into the oocyte.

In summary, we suggest that the modulation of GABAρ_1 receptor currents by lanthanides is mediated by kinetic states that have not been previously described and proposed two models for the gating of these receptors. Although they do not discard alternative kinetic schemes, these models closely reproduce the experimental results and could explain in a simple way a general mechanism for lanthanide action on GABAρ_1 receptors.

We thank Drs Cecilia Bouzat and Richard D. Nathan for their comments on the manuscript and Drs Ataúlfo Martínez-Torres and Ricardo Miledi for ρ_1 cDNA. This work was supported by FONCyT Grants PICT 5-6800 and 5-13317, BID 1201 and by NIH R01-HL57832. We also thank Pew Foundation, IBRO and Laboratorios Temis-Lostaló for support.

References

ACUNA-CASTILLO, C., MORALES, B. & HUIDOBRO-TORO, J.P. (2000). Zinc and copper modulate differentially the P2X4 receptor. *J. Neurochem.,* **74,** 1529–1537.

ARAKAWA, O., NAKAHIRO, M. & NARAHASHI, T. (1991). Mercury modulation of GABA-activated chloride channels and non-specific cation channels in rat dorsal root ganglion neurons. *Brain Res.,* **551,** 58–63.

BARBERIS, A., CHERUBINI, E. & MOZRZYMAS, J.W. (2000). Zinc inhibits miniature GABAergic currents by allosteric modulation of GABAA receptor gating. *J. Neurosci.,* **20,** 8618–8627.

BIANCHI, M.T. & MACDONALD, R.L. (2001). Agonist trapping by GABAA receptor channels. *J. Neurosci.,* **21,** 9083–9091.

CALVO, D.J. & MILEDI, R. (1995). Activation of GABA rho 1 receptors by glycine and beta-alanine. *Neuroreport,* **6,** 1118–1120.

CALVO, D.J., VAZQUEZ, A.E. & MILEDI, R. (1994). Cationic modulation of rho 1-type gamma-aminobutyrate receptors expressed in *Xenopus* oocytes. *Proc. Natl. Acad. Sci. U.S.A.,* **91,** 12725–12729.

CHANG, Y., AMIN, J. & WEISS, D.S. (1995). Zinc is a mixed antagonist of homomeric rho 1 gamma-aminobutyric acid-activated channels. *Mol. Pharmacol.,* **47,** 595–602.

CHANG, Y. & WEISS, D.S. (1999). Channel opening locks agonist onto the GABAC receptor. *Nat. Neurosci.,* **2,** 219–225.

COLQUHOUN, D. & HAWKES, A.G. (1977). Relaxation and fluctuations of membrane currents that flow through drug-operated channels. *Proc. Roy. Soc. London B Biol. Sci.,* **199,** 231–262.

COLQUHOUN, D. & HAWKES, A.G. (1981). On the stochastic properties of single ion channels. *Proc. Roy. Soc. London B Biol. Sci.,* **211,** 205–235.

COLQUHOUN, D. & HAWKES, A.G. (1982). On the stochastic properties of bursts of single ion channel openings and of clusters of bursts. *Philos. Trans. Roy. Soc. London B Biol. Sci.,* **300,** 1–59.

COLQUHOUN, D. & HAWKES, A.G. (1995). Desensitization of *N*-methyl-D-aspartate receptors: a problem of interpretation. *Proc. Natl. Acad. Sci. U.S.A.,* **92,** 10327–10329.

DODGE JR, F.A., MILEDI, R. & RAHAMIMOFF, R. (1969). Strontium and quantal release of transmitter at the neuromuscular junction. *J. Physiol.,* **200,** 267–283.

DRAGUHN, A., VERDORN, T.A., EWERT, M., SEEBURG, P.H. & SAKMANN, B. (1990). Functional and molecular distinction between recombinant rat GABAA receptor subtypes by Zn2+. *Neuron,* **5,** 781–788.

FEIGENSPAN, A., WASSLE, H. & BORMANN, J. (1993). Pharmacology of GABA receptor Cl^- channels in rat retinal bipolar cells. *Nature,* **361,** 159–162.

FISHER, J.L. & MACDONALD, R.L. (1998). The role of an alpha subtype M2-M3 His in regulating inhibition of GABAA receptor current by zinc and other divalent cations. *J. Neurosci.,* **18,** 2944–2953.

GALZI, J.L., BERTRAND, S., CORRINGER, P.J., CHANGEUX, J.P. & BERTRAND, D. (1996). Identification of calcium binding sites that regulate potentiation of a neuronal nicotinic acetylcholine receptor. *EMBO J.,* **15,** 5824–5832.

GARCIA-COLUNGA, J. & MILEDI, R. (1997). Opposite effects of lanthanum on different types of nicotinic acetylcholine receptors. *Neuroreport,* **8,** 3293–3296.

GOUTMAN, J.D. & CALVO, D.J. (2004). Studies on the mechanisms of action of picrotoxin, quercetin and pregnanolone at the GABA rho 1 receptor. *Br. J. Pharmacol.,* **141,** 717–727.

HACKOS, D.H. & KORENBROT, J.I. (1997). Calcium modulation of ligand affinity in the cyclic GMP-gated ion channels of cone photoreceptors. *J. Gen. Physiol.,* **110,** 515–528.

HOSIE, A.M., DUNNE, E.L., HARVEY, R.J. & SMART, T.G. (2003). Zinc-mediated inhibition of GABA(A) receptors: discrete binding sites underlie subtype specificity. *Nat. Neurosci.,* **6,** 362–369.

IM, M.S., HAMILTON, B.J., CARTER, D.B. & IM, W.B. (1992). Selective potentiation of GABA-mediated Cl^- current by lanthanum ion in subtypes of cloned GABAA receptors. *Neurosci. Lett.,* **144,** 165–168.

IM, W.B., PREGENZER, J.F., ARAKAWA, O., NAKAHIRO, M. & NARAHASHI, T. (1993). Interaction of La3+ with GABAA receptors in rat cerebrocortical membranes as detected with [^{35}S]t-butylbicyclophosphorothionate binding. *Eur. J. Pharmacol.,* **245,** 111–117.

LAUBE, B., KUHSE, J., RUNDSTROM, N., KIRSCH, J., SCHMIEDEN, V. & BETZ, H. (1995). Modulation by zinc ions of native rat and recombinant human inhibitory glycine receptors. *J. Physiol.,* **483** (Part 3), 613–619.

LEGENDRE, P. & WESTBROOK, G.L. (1991). Noncompetitive inhibition of gamma-aminobutyric acidA channels by Zn. *Mol. Pharmacol.,* **39,** 267–274.

MA, J.Y. & NARAHASHI, T. (1993a). Enhancement of gamma-aminobutyric acid-activated chloride channel currents by lanthanides in rat dorsal root ganglion neurons. *J. Neurosci.,* **13,** 4872–4879.

MA, J.Y., NARAHASHI, T., ARAKAWA, O. & NAKAHIRO, M. (1993b). Differential modulation of GABAA receptor-channel complex by polyvalent cations in rat dorsal root ganglion neurons. *Brain Res.,* **607,** 222–232.

MA, J.Y., REUVENY, E. & NARAHASHI, T. (1994). Terbium modulation of single gamma-aminobutyric acid-activated chloride channels in rat dorsal root ganglion neurons. *J. Neurosci.,* **14,** 3835–3841.

MAYER, M.L., WESTBROOK, G.L. & GUTHRIE, P.B. (1984). Voltage-dependent block by Mg2+ of NMDA responses in spinal cord neurones. *Nature,* **309,** 261–263.

MILEDI, R. & PARKER, I. (1980). Effects of strontium ions on end-plate channel properties. *J. Physiol.,* **306,** 567–577.

MILEDI, R., PARKER, I. & SUMIKAWA, K. (1989). Transplanting receptors from brain into oocytes. In: *Fidia Research Foundation Neuroscience Award Lecture*. ed. Smith, J. pp. 57–89. New York: Raven Press.

MOSS, S.J. & SMART, T.G. (2001). Constructing inhibitory synapses. *Nat. Rev. Neurosci.,* **2,** 240–250.

MOTT, D.D., WASHBURN, M.S., ZHANG, S., DINGLEDINE, R.J., HACKOS, D.H. & KORENBROT, J.I. (2003). Subunit-dependent modulation of kainate receptors by extracellular protons and polyamines. *J. Neurosci.,* **23,** 1179–1188.

MOZRZYMAS, J.W., ZARNOWSKA, E.D., PYTEL, M. & MERCIK, K. (2003). Modulation of GABA(A) receptors by hydrogen ions reveals synaptic GABA transient and a crucial role of the desensitization process. *J. Neurosci.,* **23,** 7981–7992.

NARAHASHI, T. (2000). Neuroreceptors and ion channels as the basis for drug action: past, present, and future. *J. Pharmacol. Exp. Ther.,* **294,** 1–26.

NARAHASHI, T., MA, J.Y., ARAKAWA, O., REUVENY, E. & NAKAHIRO, M. (1994). GABA receptor-channel complex as a target site of mercury, copper, zinc, and lanthanides. *Cell Mol. Neurobiol.,* **14,** 599–621.

POLENZANI, L., WOODWARD, R.M. & MILEDI, R. (1991). Expression of mammalian gamma-aminobutyric acid receptors with distinct pharmacology in *Xenopus* oocytes. *Proc. Natl. Acad. Sci. U.S.A.,* **88,** 4318–4322.

QIAN, H., LI, L., CHAPPELL, R.L. & RIPPS, H. (1997). GABA receptors of bipolar cells from the skate retina: actions of zinc on GABA-mediated membrane currents. *J. Neurophysiol.,* **78,** 2402–2412.

RAGOZZINO, D., WOODWARD, R.M., MURATA, Y., EUSEBI, F., OVERMAN, L.E. & MILEDI, R. (1996). Design and *in vitro* pharmacology of a selective gamma-aminobutyric acidC receptor antagonist. *Mol. Pharmacol.,* **50,** 1024–1030.

REICHLING, D.B. & MACDERMOTT, A.B. (1991). Lanthanum actions on excitatory amino acid-gated currents and voltage-gated calcium currents in rat dorsal horn neurons. *J. Physiol.,* **441,** 199–218.

ROSALES, R.A., FILL, M. & ESCOBAR, A.L. (2004). Calcium regulation of single ryanodine receptor channel gating analyzed using HMM/MCMC statistical methods. *J. Gen. Physiol.,* **123,** 533–553.

SAXENA, N.C., NEELANDS, T.R. & MACDONALD, R.L. (1997). Contrasting actions of lanthanum on different recombinant gamma-aminobutyric acid receptor isoforms expressed in L929 fibroblasts. *Mol. Pharmacol.,* **51,** 328–335.

SMART, T.G. (1992). A novel modulatory binding site for zinc on the GABAA receptor complex in cultured rat neurones. *J. Physiol.,* **447,** 587–625.

SMART, T.G. & CONSTANTI, A. (1982). A novel effect of zinc on the lobster muscle GABA receptor. *Proc. Roy Soc. London B Biol. Sci.,* **215,** 327–341.

SQUIRES, R.F. & SAEDERUP, E. (1982). gamma-aminobutyric acid receptors modulate cation binding sites coupled to independent benzodiazepine, picrotoxin, and anion binding sites. *Mol. Pharmacol.,* **22,** 327–334.

WANG, T.L., HACKAM, A.S., GUGGINO, W.B. & CUTTING, G.R. (1995). A single amino acid in gamma-aminobutyric acid rho 1 receptors affects competitive and noncompetitive components of picrotoxin inhibition. *Proc. Natl. Acad. Sci. U.S.A.,* **92,** 11751–11755.

WESTBROOK, G.L. & MAYER, M.L. (1987). Micromolar concentrations of Zn2+ antagonize NMDA and GABA responses of hippocampal neurons. *Nature,* **328,** 640–643.

WOODWARD, R.M., POLENZANI, L. & MILEDI, R. (1992). Characterization of bicuculline/baclofen-insensitive gamma-aminobutyric acid receptors expressed in *Xenopus* oocytes. I. Effects of Cl− channel inhibitors. *Mol. Pharmacol.,* **42,** 165–173.

WOTRING, V.E., CHANG, Y. & WEISS, D.S. (1999). Permeability and single channel conductance of human homomeric rho1 GABAC receptors. *J. Physiol.,* **521** (Part 2), 327–336.

ZHU, W.J., WANG, J.F., CORSI, L. & VICINI, S. (1998). Lanthanum-mediated modification of GABAA receptor deactivation, desensitization and inhibitory synaptic currents in rat cerebellar neurons. *J. Physiol.,* **511** (Part 3), 647–661.

(Received May 31, 2005
Revised June 28, 2005
Accepted September 5, 2005
Published online 10 October 2005)